NEURAL REGENERATION RESEARCH
October 2016, Volume 11, Issue 10
www.nrronline.org

RESEARCH ARTICLE

Preparation of polypyrrole-embedded electrospun poly(lactic acid) nanofibrous scaffolds for nerve tissue engineering

Jun-feng Zhou[1, #], Yi-guo Wang[2, 3, #], Liang Cheng[1], Zhao Wu[1], Xiao-dan Sun[1, *], Jiang Peng[2, 4, *]

1 Key Laboratory of Advanced Materials of Ministry of Education of China, School of Materials Science and Engineering, Tsinghua University, Beijing, China
2 Institute of Orthopedics, Chinese PLA General Hospital, Beijing, China
3 School of Medicine, Nankai University, Tianjin, China
4 The Neural Regeneration Co-innovation Center of Jiangsu Province, Nantong, Jiangsu Province, China

How to cite this article: *Zhou JF, Wang YG, Cheng L, Wu Z, Sun XD, Peng J (2016) Preparation of polypyrrole-embedded electrospun poly(lactic acid) nanofibrous scaffolds for nerve tissue engineering. Neural Regen Res 11(10):1644-1652.*

Funding: *This research was financially supported by Tsinghua University Initiative Scientific Research Program, No. 20131089199; the National Key Research and Development Program of China, No. 2016YFB0700802; the National Program on Key Basic Research Project of China (973 Program), No. 2012CB518106, 2014CB542201.*

Graphical Abstract

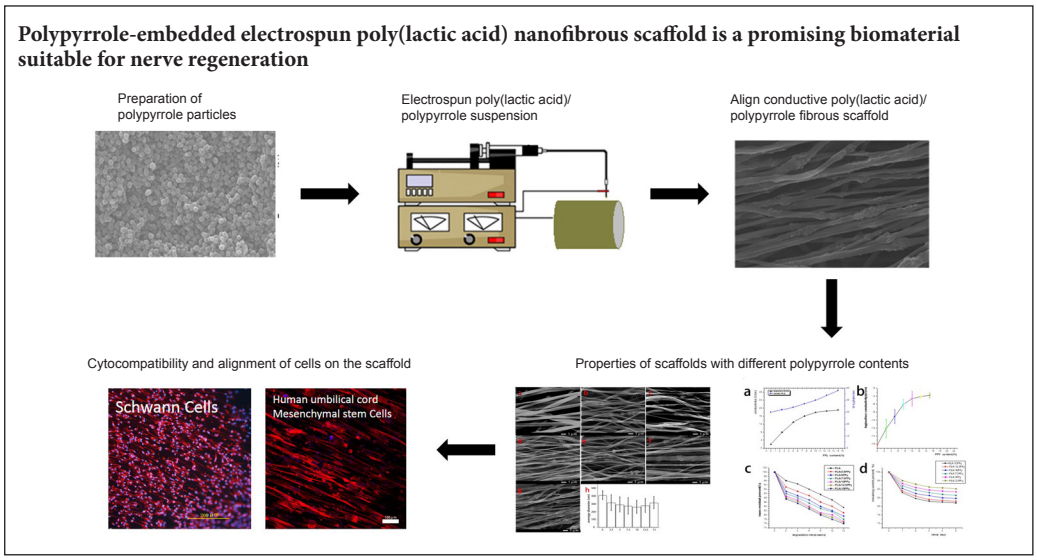

Correspondence to:
Xiao-dan Sun or Jiang Peng, sunxiaodan@mail.tsinghua.edu.cn or pengjiang301@126.com.

#These authors contributed equally to this study.

orcid:
0000-0002-5210-128X (Xiao-dan Sun)
0000-0003-4662-9288 (Jiang Peng)

doi: *10.4103/1673-5374.193245*

Accepted: *2016-09-01*

Abstract

Polypyrrole (PPy) is a biocompatible polymer with good conductivity. Studies combining PPy with electrospinning have been reported; however, the associated decrease in PPy conductivity has not yet been resolved. We embedded PPy into poly(lactic acid) (PLA) nanofibers *via* electrospinning and fabricated a PLA/PPy nanofibrous scaffold containing 15% PPy with sustained conductivity and aligned topography. There was good biocompatibility between the scaffold and human umbilical cord mesenchymal stem cells as well as Schwann cells. Additionally, the direction of cell elongation on the scaffold was parallel to the direction of fibers. Our findings suggest that the aligned PLA/PPy nanofibrous scaffold is a promising biomaterial for peripheral nerve regeneration.

Key Words: *nerve regeneration; polypyrrole; electrospinning; conductivity; electrical property; Schwann cells; human umbilical cord mesenchymal stem cells; nerve tissue engineering; nanofibrous scaffolds; neural regeneration*

Introduction

Nerve tissue repair is of great interest in human health care as it directly impacts on the quality of life (Arslantunali et al., 2014). An established approach in neural tissue engineering involves the fabrication of polymeric scaffolds with nerve cells to produce a three-dimensional functional tissue suitable for implantation (Yuan et al., 2014; Zhang et al., 2014a; Wang et al., 2015a). Electrical stimulation (ES) is a treatment for nerve regeneration and is effective for accelerating the healing rate of peripheral nerve injury (Zhang et al., 2014b). Polypyrrole (PPy) is one of the most thoroughly investigated conductive polymers because of its high electrical conductivity, flexibility of preparation, excellent environmental stability (Wang et al., 2004a), low toxicity (Wang et al., 2004a; Ramanaviciene et al., 2007) and ability to support cell adhesion and growth under ES (Sudwilai et al., 2014; Xu et al., 2014). However, the conjugated molecular structure of PPy may be damaged by dissolved oxygen in aqueous conditions and in the presence of current, resulting in a deterioration of conductivity (Meng et al., 2008). To achieve electrical conductivity stability and to improve its flexibility, processibility and biodegradability, studies have focused on blending PPy with other processable and biodegradable polymers (Wang et al., 2003; Meng et al., 2008). We combined poly(lactic acid) (PLA) and PPy in this study, because PLA has excellent pliancy and biocompatibility (Li et al., 2013; Yu et al., 2013; Sudwilai et al., 2014).

Compared with a dense membrane, a porous structure with a high surface-to-volume ratio is more suitable for biomedical applications. Electrospinning is a simple and relatively efficient technique to fabricate polymer into such a porous three-dimensional fiber network (Xie et al., 2010; Hu et al., 2012). The surface topography, including the diameter, orientation and surface roughness of electrospun nanofibers can modulate cellular activity by contact guidance (Schmidt and Leach, 2003; Corey et al., 2007; Yang et al., 2015). *In situ* polymerization and coating are the most popular strategies to prepare PPy-coated composite fibers *via* the electrospinning process (Liu et al., 2010; Pelto et al., 2013; Yu et al., 2013; Sudwilai et al., 2014). However, these *in situ* polymerized PPy layers are still at risk of losing conductivity in media (Shi et al., 2004) and are potentially toxic from residual oxidants. Studies on PPy-embedded electrospun composite fibers (Kai et al., 2011), and the effect of PPy on the formation of the composite fiber preparation and the surface topography of electrospun fibers are rare.

Biomaterials should have good compatibility with cells at the site of injury. Schwann cells are important in neural development and regeneration (Zhang et al., 2014c). After peripheral nerve injury, Schwann cells form new myelin to guide the axon back to its target and secrete bioactive molecules to boost the regeneration (Xu et al., 2016). Stem cells have great potential for peripheral nerve repair. Mesenchymal stem cells can differentiate into supporting cells, such as Schwann cells, and even undifferentiated ones can secrete neurotrophic factors for neural regeneration (Zhang et al., 2011; Sharma et al., 2016). Umbilical cord mesenchymal stem cells are isolated from the umbilical cord after birth (Guo et al., 2015). Compared with mesenchymal stem cells from other parts of the body, umbilical cord mesenchymal stem cells are more primitive, proliferative and immunosuppressive. Umbilical cord stem cells were proposed as a potential new "gold standard" for mesenchymal stem cell-based therapy (El Omar et al., 2014).

In this study, we prepared electrospun PLA/PPy nanofibers, and analyzed their properties, observed their biocompatibility and explored their effectiveness for nerve repair.

Materials and Methods

Synthesis and characterization of PPy particles

Spherical PPy nanoparticles were synthesized using chemical polymerization with P123 ($EO_{20}PO_{70}EO_{20}$, Ma = 5,800) as a template agent. In brief, 2.3 g P123 (Sigma-Aldrich, St. Louis, Missouri, USA) was dissolved in 230 mL deionized water at 40°C for 3 hours and then cooled to room temperature. Pyrrole (98%, Sinopharm Chemical Reagent Co., Shanghai, China) was distilled under reduced pressure and stored in a refrigerator at 4°C prior to use. Then, pyrrole monomer (0.1 M, 1,590 μL) was added to the P123 solution. One hour later, $FeCl_3 \bullet 6H_2O$ (0.3 M, 18.65 g, Beijing Chemical Works, China) was added into the solution and the polymerization temperature was maintained at 18°C. The mixture solution turned black within a few minutes and was stirred for 6 hours. The formed PPy precipitate was then collected by centrifugation and was washed several times with deionized water and ethanol (Beijing Chemical Works, China). It was then dried under a vacuum atmosphere at 60°C for 24 hours and ground to a fine powder for future use.

The morphology of the PPy particles was observed by field emission scanning electron microscopy (FE-SEM, HITACHI, Tokyo, Japan, S-5500, 5.0 kV). The diameter of 100 randomly chosen single PPy particles, which were lying flat on the sample holder, was measured using image analysis (Photoshop CS5, Adobe System Inc., San Jose, California, USA) from a randomly selected FE-SEM image. The conductivity of PPy powders was measured with compressed pellets using the standard four-probe method at room temperature.

Preparation and characterization of the PLA/PPy electrospun suspensions

The PPy nanoparticles were dispersed ultrasonically in N,N-dimethylformamide (DMF; Beijing Chemical Works) at different concentrations for 2 hours and then stirred continuously overnight at room temperature. PLA with an average molecular weight (Mw) of 130,000 g/mol (inherent viscosity 0.97 dL/g) was supplied by Shandong Institute of Medical Instruments, Jinan, Shandong, China. PLA at a concentration of 15% (w/v) was dissolved in dichloromethane (DCM; Beijing Chemical Works) at room temperature. PLA solution was added to the above PPy dispersions to achieve various PPy content ratios (0%, 2.5%, 5%, 7.5%, 10%, 12.5% and 15%) and stirred for 24 hours to achieve homogeneous PLA/PPy suspensions [v(DMF):v(DCM) = 1:4].

Conductivity of the suspensions at different PPy concentrations was measured with a digital conductivity meter (DDS-12A, Chinainhy, Shanghai, China). A Physica MCR 301 rheometer (Anton Paar GmbH, Graz, Austria) with a cone-plate measuring system was used to evaluate the rheological properties of composite suspensions under a share rate of 4 s^{-1}, which was the estimated rate for the beginning of electrospinning. All measurements were performed before electrospinning.

Electrospinning

The electrospinning apparatus is shown in **Figure 1**. The prepared suspensions were placed in a 20 mL plastic syringe with a stainless steel needle of inner diameter 1.2 mm. A collecting drum rotating at a speed of approximately 3,000 r/min was used as the collector. A positive DC high-voltage power supply (Spellman, SL150, New York, USA) was connected to the needle to generate a high electric field of 1.0 kV/cm between the capillary tube and the grounded collector at a distance of 20 cm. Feeding rate of the solution was 0.8 mL/hour. Pure PLA nanofibers were fabricated using the similar method. The electrospun scaffolds were dried under vacuum at room temperature for 3 days before they were characterized. The pure PLA nanofiber scaffolds and the composite PLA/PPy nanofiber scaffolds were denominated as PLA, PLA/2.5PPy, PLA/5PPy, PLA/7.5PPy, PLA/10PPy, PLA/12.5PPy and PLA/15PPy corresponding to PPy weight ratios of 0%, 2.5%, 5%, 7.5%, 10%, 12.5% and 15%, respectively.

Characterization of nanofiber scaffolds

Scanning electron microscopy

The electrospun pure PLA and composite PLA/PPy nanofiber scaffolds were gold-coated using sputter coating to observe the surface topographies using scanning electron microscopy (FEI, Quanta 200, Philips, Eindhoven, Netherlands). The electron accelerating voltage was 20.0 kV. Micrographs from the scanning electron microscope analysis were digitized and analyzed using Image Tool 2.0 (Fudan University, Shanghai, China) to determine the average fiber diameter of the nanofibers produced. Fifty points on fibers were selected from one image. Fiber diameter at these points was measured to determine the diameter distribution. To select the points where fiber diameter was measured, several lines were drawn randomly on the images and the middle point of the intersections of the lines and fibers were chosen as the points to be analyzed.

Transmission electron microscopy

The dispersion of PPy nanoparticles coated in the composite nanofibers were observed by transmission electron microscope (Hitachi H-700H, Tokyo, Japan) at the electron acceleration voltage of 150 kV. The nanofiber samples were prepared by directly electrospinning the PLA/PPy solution onto copper grids for about 50 seconds, and were then dried under vacuum immediately over 24 hours to completely remove residual solvent.

Electrical properties

The surface conductivity measurements of the scaffolds were performed using a ZC36 high resistance meter (Shanghai Precision Instrument Co., Shanghai, China) at ambient temperature. The scaffolds were cleaned with ethanol and dried at 55°C before measurement. At least five specimens were measured for each sample and the reported results were the average values.

Degradation of fiber scaffolds in PBS

The nanofiber scaffolds were cut into small square pieces with original mass (w_0) of 0.5 g, and placed in 1 mL phosphate buffered saline (PBS) (pH 7.4) at 37°C for 12 weeks. Every 2 weeks, triplicate specimens for each nanofiber mesh were retrieved from PBS and rinsed with deionized water to remove residual buffer salts before they were dried to constant weight (w). The mass loss was determined by equation (1):

$$Mass\ residual\ percent = \frac{\omega}{\omega_0} \times 100\% \quad (1)$$

Electrical stability of fiber scaffolds in PBS

Electrical stability is defined as the remaining percentage of electrical conductivity (γ) of the conductive scaffolds, as the electrical stability test proceeds. The PLA/PPy composite scaffolds were cut into rectangular specimens of 2.0 × 2.0 cm in size and incubated in 5 mL PBS at pH = 7.4 at 37°C for 5 days. A constant electrical potential (U) of 100 mV/cm was applied across the opposite sides of the specimens for 2 hours every day using an electrochemical workstation (CHI600C, Shanghai Chenhua Instrument Co., Shanghai, China). Electrical current (I) passing through the membranes was recorded every day from the beginning of applying electrical potential. The remaining conductivity of the specimens was calculated by equation (2), where γ was the conductivity of the scaffolds and $\Delta\gamma$ and ΔI were the changes of γ and I.

$$\text{The remaining conductivity percent} = 1-\frac{\Delta\gamma}{\gamma} = 1-\frac{\Delta I}{I}$$

$$= \text{the remaining current percent} \quad (2)$$

***In vitro* experiments**

Isolation of Schwann cells

Schwann cells were isolated from the sciatic nerve of Sprague-Dawley rats aged 3 days [Animal Center of Chinese PLA 307 Hospital, Beijing, China; license No. SCXK-(Army)-2012-0004], Sciatic nerves were cut into small fragments and enzymatically dissociated in 1% collagenase (Sigma-Aldrich, St. Louis, MI, USA) for 30 minutes. Dulbecco's modified Eagle's medium/nutrient Mixture F-12 (DMEM/F12; Gibco-Invitrogen, Thermo Fisher Scientific, Carlsbad, CA, USA) containing 10% fetal bovine serum (FBS; Gibco-Invitrogen) was prepared as culture medium. The cell suspension was stirred, centrifuged and incubated in culture medium. Twenty-four hours later, the culture medium was replaced with culture media supplemented with 50 ng/mL cytosine arabinoside (Ara-C) (Sigma-Aldrich) to remove fibroblasts (Gu et al., 2012). After anoth-

er 24 hours, the cells were incubated in culture medium containing 2 nM forskolin (Sigma-Aldrich) and 2 ng/mL heregulin (Sigma-Aldrich) to accelerate cell proliferation. Purity of cells was assessed by immunostaining with S100 (Kim et al., 2008). Cultures with purity above 95% were used for the following assays.

Schwann cell culture and immunohistochemical staining

The PLA/15PPy scaffolds were fixed to the bottom of wells of six-well plates and sterilized with ^{60}Co radiation. The scaffold was soaked in medium for 24 hours at 37°C prior to plating. 1.5×10^5 Schwann cells were seeded onto the scaffolds and cultured for 5 days. Schwann cells cultured on the tissue culture plates (TCPs) were a control group. For immunohistochemical staining, samples were rinsed twice in PBS and then fixed in 4% paraformaldehyde for 30 minutes. Samples were then permeabilized and blocked in 0.1% Triton-X100 with 10% goat serum for 30 minutes. After rinsing twice in PBS, samples were incubated with mouse primary antibody S100 (1: 200; Sigma-Aldrich) overnight at 4°C and then incubated with rabbit primary antibody P75 (1:200; Sigma-Aldrich overnight at 4°C. Alexa Fluor 488-conjugated goat anti-mouse antibody (1:500; ZSGB-BIO, Beijing, China) and Alexa Fluor 594-conjugated goat anti-rabbit antibody (1:500; ZSGB-BIO) were used as secondary antibodies to S100 and P75, respectively. DAPI (Bio-topped Co., Beijing, China) was used to stain nuclei. The stained samples were visualized by laser scanning confocal microscope (Zeiss LSM 780, Oberkochen, Germany). Samples on the scaffolds and controls stained only with S100 and Alexa Fluor 594-conjugated goat anti-mouse antibody (1:500; ZSGB-BIO) secondary antibody and DAPI were visualized by fluorescence microscopy (Olympus, Tokyo, Japan). Cell number density was counted from three different views of images and cell orientation was quantified by measuring the angles between the major neurite axis and the fiber axis.

Human umbilical cord mesenchymal stem cell culture and immunofluorescent staining

Human umbilical cord mesenchymal stem cells (Cyagen Biosciences Inc., Santa Clara, CA, USA) were cultured in alpha-minimum essential medium (α-MEM; Bio-topped Co., Beijing, China) containing 9% FBS and 1% penicillin and streptomycin (PS; Bio-topped Co.). The scaffold was soaked in the medium for 24 hours at 37°C prior to plating. 1.5×10^5 cells of passage 5 were used to seed the PLA/15PPy nanofibrous scaffolds. After culture for 5 days, human umbilical cord stem cells were rinsed twice in PBS and then fixed in 4% paraformaldehyde for 30 minutes and then permeabilized in 0.1% Triton-X100. Cells were then rinsed twice and incubated in phalloidin-rhodamine solutions for 45 minutes, followed by staining with DAPI. The samples were observed with laser scanning confocal microscope (Zeiss LSM 780).

Statistical analysis

Data are expressed as the mean ± SD, and statistical analysis was performed by one-way analysis of variance (Microsoft Excel 2013, Redmond, Washington State, USA or OriginPro 8, OriginLab, Northanmpton, MA, USA) unless stated. Differences were considered significant at $P < 0.05$.

Results

Characterization of PPy nanoparticles

As shown in **Figure 2**, PPy nanoparticles demonstrated spherical shapes with the diameter distributed uniformly at 92 ± 15 nm. The electrical conductivity of the PPy tablets was 4.6 s/cm.

Morphology of electrospun nanofibers

Figure 3 shows typical morphology of the electrospun nanofibers containing PPy nanoparticles. The PPy nanoparticles were dispersed within the fiber networks on a large scale (**Figure 3A**, **C**). PPy nanoparticles were located in the nanofibers, causing a rough fiber surface (**Figure 3D**). A quantitative analysis of fiber diameter distribution is given in **Figure 4B**, and presents a normal distribution. The average fiber diameter was 320.7 ± 83.0 nm, which is bigger than that of PPy nanoparticles, so indicates the embedding of PPy nanoparticles.

PPy weight ratios in composite PLA/PPy nanofiber scaffolds

As seen from **Figure 4**, SEM images of the final nanofiber scaffolds revealed the effects of PPy content on nanofiber topographic features, including nanofiber diameters and surface roughness. It can be observed that pure PLA nanofibers were smooth in appearance (**Figure 4A**), while the surface of composite PLA/PPy nanofibers became rougher as PPy content increased. The average diameters of pure PLA nanofibers were about 415 nm, while they decreased dramatically to about 319 nm for PLA/2.5PPy. Furthermore, as the PPy content in the PLA nanofibers increased, the diameters showed a gradual linear decrease to approximately 296 nm, 277 nm, and 265 nm for PLA/5PPy, PLA/7.5PPy and PLA/10PPy, respectively. However, when the PPy content reached or exceeded 12.5%, the nanofiber diameters increased slightly, and the diameters of PLA/12.5PPy and PLA/15PPy were approximately 283 and 320 nm respectively, which were still smaller than that of pure PLA nanofibers.

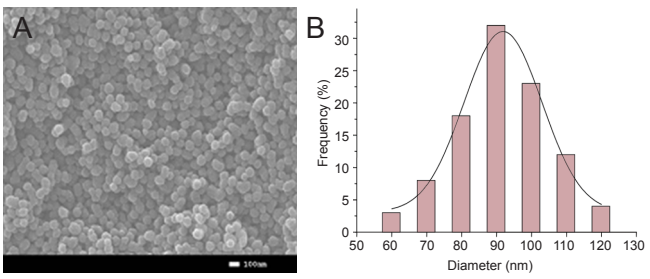

Figure 2 Morphology of polypyrrole (PPy) nanoparticles.
(A) Scanning electron microscope image of PPy nanoparticles. Scale bar: 100 nm. (B) Distribution histogram of PPy nanoparticle diameter. The fitting Gaussian distribution curve is also shown on the graph.

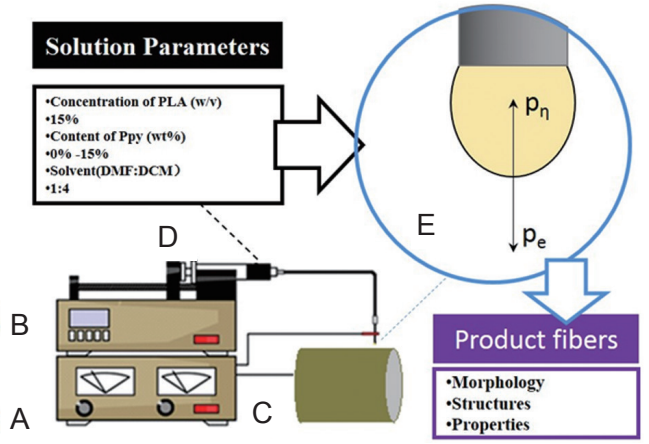

Figure 1 Illustration of the electrospinning apparatus.
(A) High-voltage power supply, (B) feeding pump, (C) grounded collector, (D) syringe and composite suspension, and (E) force analysis for formation of spinning jet. p_e: Electric field stress; p_η: visco elastic stress; PLA: poly(lactic acid); PPy: polypyrrole; DMF: N,N-dimethylformamide; DCM: dichloromethane.

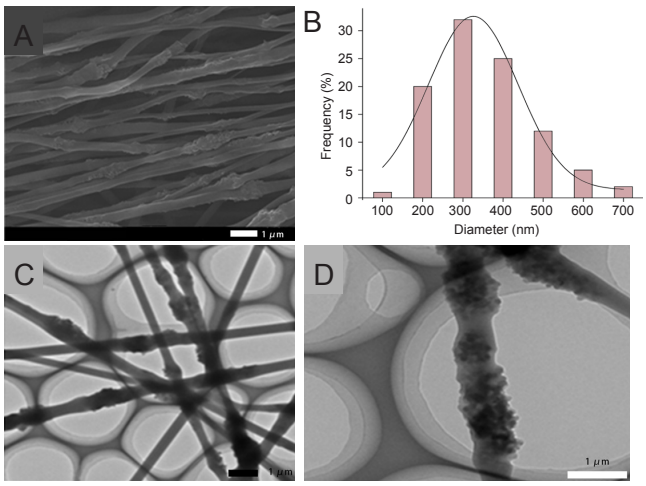

Figure 3 Morphology of the electrospun nanofibers containing PPy nanoparticles.
(A) SEM images of the electrospun nanofibers (15% w/v PLA, 10 wt% PPy, DMF/DCM = 1:4), (B) histograms of fiber diameter distribution, and (C, D) TEM images of PLA/10PPy. Scale bars: 1 μm. PPy: Polypyrrole; SEM: scanning electron microscope; DMF: N,N-dimethylformamide; DCM: dichloromethane: TEM: transmission electron microscope; PLA: poly(lactic acid).

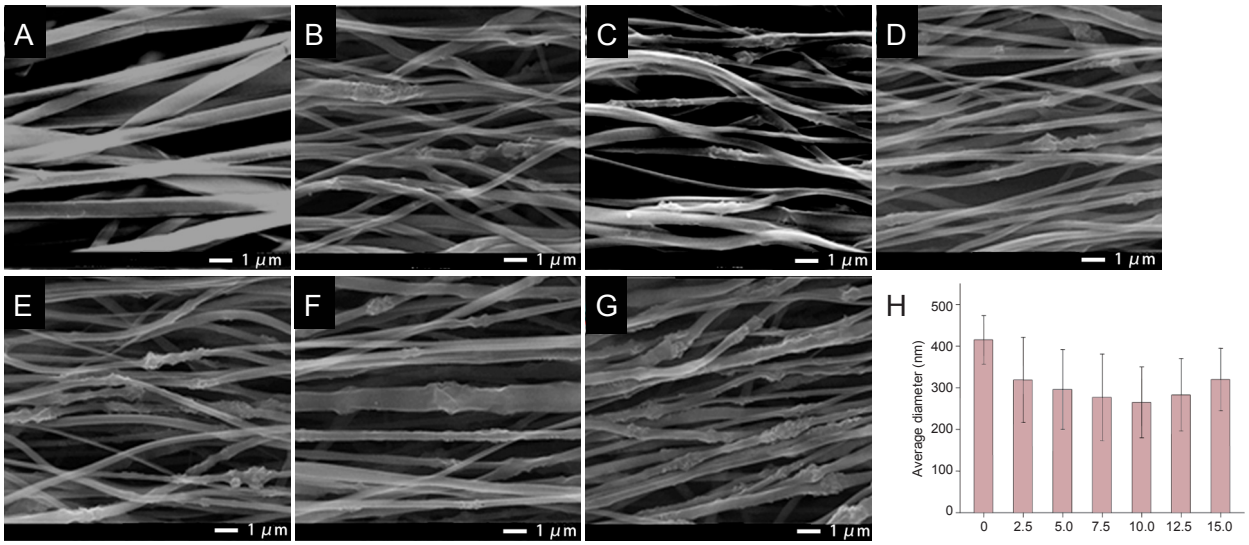

Figure 4 Morphology of PLA/PPy electrospun nanofibers.
(A–G) SEM images of PLA/PPy electrospun nanofibers with various PPy contents: 0%, 2.5%, 5%, 7.5%, 10%, 12.5% and 15% (scale bars: 1 μm) and (H) quantitative analysis of average fiber diameters. PLA: Poly(lactic acid); PPy: polypyrrole; SEM: scanning electron microscope.

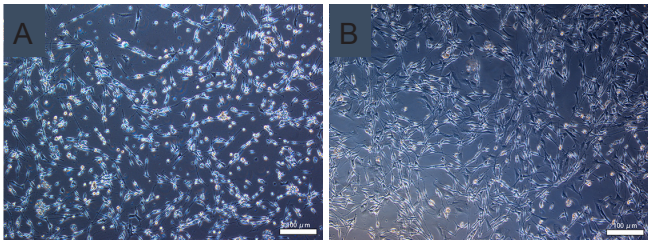

Figure 6 Morphology of primary Schwann cells and purified Schwann cells (inverted microscopy).
(A) Schwann cells accompanied by fibroblasts. (B) Purified Schwann cells showed a typical spindle-like shape. Bars: 100 μm.

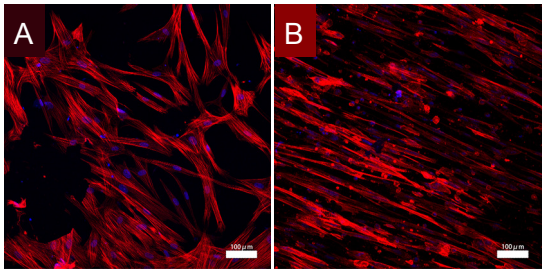

Figure 9 Human umbilical cord mesenchymal stem cells.
Cells cultured on (A) TCP and (B) PLA/15PPy. Blue: DAPI; Red: phalloidin-rhodamine; Bars: 100 μm. TCP: Tissue culture plate; PLA: poly(lactic acid); PPy: polypyrrole.

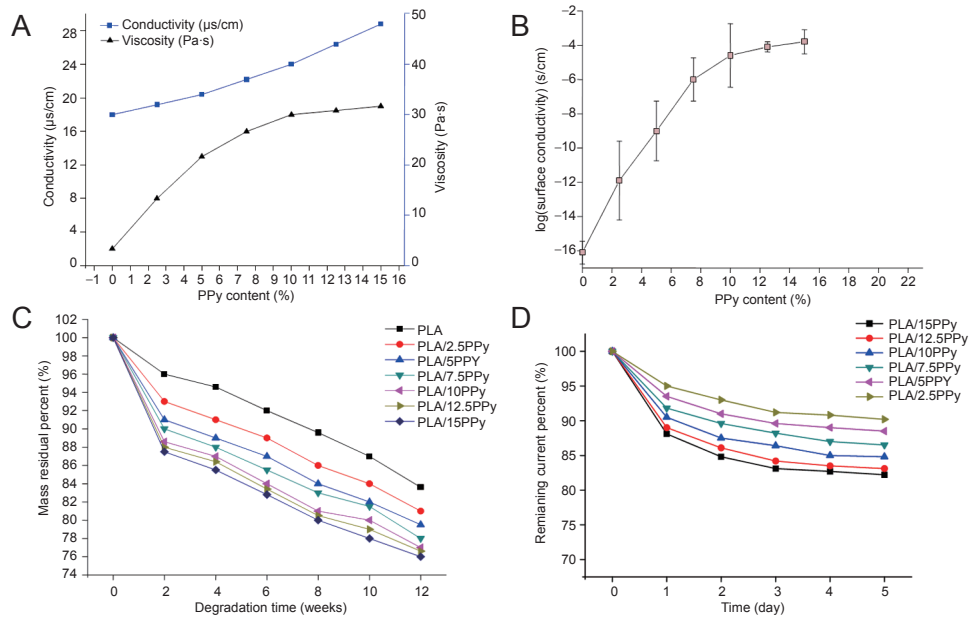

Figure 5 Properties of suspensions.
(A) Conductivity (black lines) and viscosity (blue lines) *vs.* PPy content in suspension. (B) Effect of PPy particle content on the surface conductivity of electrospun composite PLA/PPy nanofiber scaffolds. (C) *In vitro* degradation of electrospun nanofiber scaffolds in PBS (pH 7.4) at 37°C. (D) The electrical stability test of PLA/PPy nanofiber scaffolds. PPy: Polypyrrole; PLA: poly(lactic acid); PBS: phosphate buffered saline.

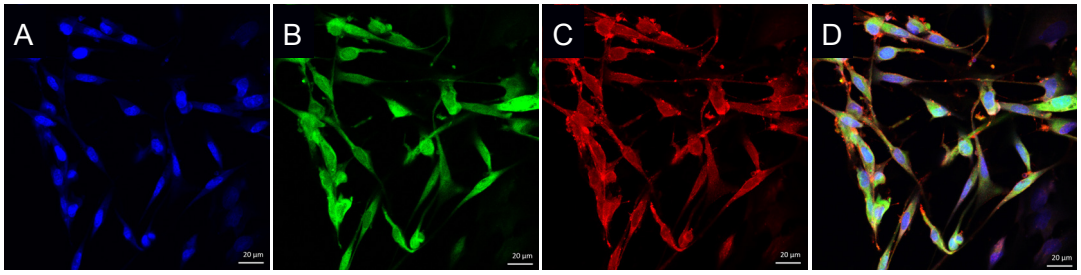

Figure 7 Immunocytochemical identification of Schwann cells.
(A) DAPI staining (blue). (B) Cells positive for S100 (Alexa Fluor 488: green). (C) Cells positive for P75 (Alexa Fluor 594: red). (D) Merged image of (A), (B) and (C). Bars: 20 μm.

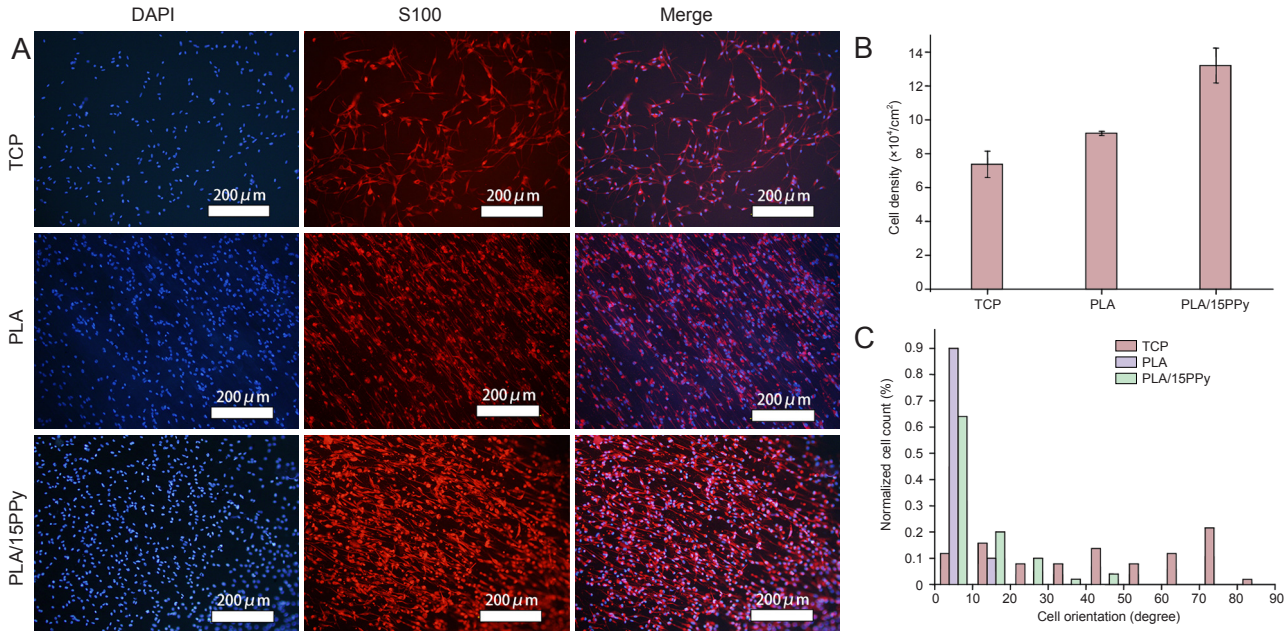

Figure 8 Number and distribution of Schwann cells on TCP, PLA and PLA/15PPy nanofibrous scaffolds.
(A) S100 immunostaining of Schwann cells on TCP, PLA and PLA/15PPy scaffolds. DAPI staining: blue; S100 staining: Alexa Fluor 594, red. Bars: 200 μm. (B) Cell density. (C) Cell orientation distribution. PLA: Poly(lactic acid); PPy: polypyrrole; TCP: tissue culture plate.

Properties of suspensions

As indicated in **Figure 5A**, the conductivity and viscosity of the suspensions increased with the addition of PPy nanoparticles. When PPy content was below 10%, the suspension conductivity increased by approximately 4, 6, 8, and 9 times for PLA/2.5PPy, PLA/5PPy, PLA/7.5PPy, and PLA/10PPy, respectively; while the viscosity of the suspension only increased by up to 1.6 times compared with pure PLA solutions.

Electrical properties of fiber scaffolds

The surface conductivity of pure PLA fiber scaffolds was lower than 1×10^{-16} s/cm, which is thought to be complete insulation. With the addition of PPy nanoparticles, the surface conductivity of the PLA/PPy scaffolds gradually increased with increasing content of PPy and exhibited a typical electrical percolation at approximately 7%, where the surface conductivity was as high as 1×10^{-6} s/cm, as shown in **Figure 5B**. Above 10%, the increase of surface conductivity was moderate, and the surface conductivity magnitude of PLA/12.5PPy and PLA/15PPy reached 1×10^{-4} s/cm. However, no significant differences were observed among PLA/10PPy, PLA/12.5PPy and PLA/15PPy in surface conductivity ($P > 0.05$).

Degradation of fiber scaffolds in PBS

As shown in **Figure 5C**, the mass of the PLA/PPy nanofibrous scaffolds decreased gradually over the incubation period, and the mass lost was faster with greater PPy content in the scaffolds. PLA nanofibrous scaffolds lost 14% of their weight while the one with most PPy, PLA/15PPy, lost 24%.

Electrical stability of fiber scaffolds in PBS

As illustrated in **Figure 5D**, conductivity of all the samples declined relatively fast on the first day, then it declined at a much slower speed over the following 4 days. On the 5th day, the remaining percentage of conductivity was 82%, 83%, 84.7%, 86.5%, 88.5%, and 90.3% for PLA/15PPy, PLA/12.5PPy, PLA/10PPy, PLA/7.5PPy, PLA/5PPy, and PLA/2.5PPy scaffolds, respectively, which indicated a stable electrical property for PLA/PPy nanofibrous scaffolds in PBS.

***In vitro* experiments of Schwann cells and human umbilical cord mesenchymal stem cells**

Isolated Schwann cells were considered as primary Schwann cells and were accompanied by fibroblasts, as shown in **Figure 6A**. Purified Schwann cells showed a typical spindle-like shape under a phase contrast microscope (**Figure 6B**). These cells all stained with S100 and P75, which are specific markers for Schwann cells (**Figure 7**), indicating efficient purification. Cells exhibited better attachment to PLA/15PPy nanofibrous scaffolds than to PLA nanofibrous scaffolds (**Figure 8A**, **B**). Schwann cells stained with S100 showed neuritis aligning with PLA and PLA/15PPy nanofibers (**Figure 8A**). **Figure 8C** illustrates that 90% of cells on nanofibers were aligned to within 30 degrees while cell orientation ranged from 0 to 90 degrees on TCPs.

Figure 9 illustrates that, similar to Schwann cells, human umbilical cord stem cells attached strongly to the PLA/15PPy nanofibrous scaffolds. The cell bodies were uniformly aligned along the nanofibers.

Discussion

Among the numerous attempts to integrate tissue-engineering concepts into strategies to repair nearly all parts of the body, neuronal repair stands out. This is partially owing to the complexity of the anatomy and functioning of the nervous system and to the inefficiency of conventional repair approaches, which are based on single components of either biomaterials or cells alone (Zhang et al., 2005). Recently, electrospun nanofibrous scaffolds have been used for nerve tissue engineering (Murugan and Ramakrishna, 2007).

In this study, we prepared aligned conductive PLA/PPy nanofibrous scaffolds that contain different amounts of PPy nanoparticles *via* electrospinning. PPy nanoparticles with a diameter of 92 nm were prepared for easy embedding. With different PPy nanoparticle ratios, the diameter of the electrospun nanofibers varied around 300 nm. The conductivity of the PLA/PPy fiber scaffolds increased with increasing PPy content. When the PPy nanoparticle content was above 10%, the conductivity was 1×10^{-5} s/cm. Furthermore, by embedding PPy nanoparticles into PLA nanofibers, the PLA/PPy scaffolds maintained at least 80% conductivity for five days. *In vitro* tests showed that aligned PLA and PLA/PPy nanofibers, fabricated by electrospinning, provided a scaffold for the controlled orientation for Schwann cells and human umbilical cord stem cells. This demonstrates that the aligned electrospun nanofibers are capable of controlling the orientation of cells by a mechanism called contact guidance (Zhang et al., 2005). The direction of cell elongation was parallel to the direction of fiber alignment and such contact guidance might enhance the nerve regeneration process.

Electrospinning mimics the structure of the extracellular matrix, which facilitates cell attachment and proliferation (Wang et al., 2015b). However, fiber morphology and the diameter of the networks are affected by several factors. In theory, a continuous jet can issue from the tip of the fluid cone (Taylor cone) when the electric field force stress (p_e) can overcome the visco elastic stress (p_η) during electrospinning. As the p_e/p_η ratio increases,the diameter of nanofibers decreases (Hohman et al., 2001a, b; Shin et al., 2001). Under certain processing conditions, these forces mainly depend on the physical properties of the solutions/suspensions (Zong et al., 2002; Liu et al., 2008). Therefore, suspension properties like viscosity and conductivity, which are determined by the suspension compositions, can be essential factors in the determination of fiber morphology. Here, the addition of PPy was the only factor that changed the conductivity and viscosity of the suspension. The conductivity of the suspension increased along with the increase in PPy content. With the rapid increase of suspension conductivity, p_e also increased. Meanwhile, the suspension viscosity did not increase greatly at these PPy contents. Therefore, it appeared that the diameter of nanofibers decreased with the increase of PPy con-

tent. When PPy content was above 10%, the increase of the suspension conductivity was moderate, while the viscosity increased more rapidly with the increase in PPy content. Therefore, p_η increased more than p_e, and it appeared that the diameter of nanofibers increased.

It was reported that electrospun nanofibers with very small diameters degrade rapidly owing to a relatively large surface area (Shao et al., 2011). As described above, the diameter of composite PLA/PPy nanofibers decreased as PPy content rose from 2.5% to 10%. When PPy content was above 10%, the surface of PLA/PPy nanofibers became very rough. The rough nanofiber surface increased the contact surface area between the polymer and water, consequently accelerating matrix breakdown.

The stability of polypyrrole conductivity was investigated by Zhang's group (Zhang et al., 2007). They studied a series of biodegradable conductive composite membranes formed by embedding PPy nanospherical particles into an insulated poly(D,L-lactide) (PDLA) matrix (Shi et al., 2004; Wang et al., 2004a; b; Zhang et al., 2007; Stewart et al., 2012). These membranes showed good conductivity and improvement of electrical stability compared with PPy when exposed to media. The composite membranes were also demonstrated to stimulate the growth of fibroblasts (Shi et al., 2004; Zhang et al., 2007) and PC12 cells (Wang et al., 2004b). However, their membranes were prepared by solvent evaporation which resulted in dense membranes without designed surface to pography. In our work, the composite demonstrated stable conductivity similar to that of Zhang et al. (2007). We took advantage of their mixture strategy in our study while incorporating specific surface topography for better biological application.

Surface topography is of great importance for the interaction between biomaterials and cells (Xie et al., 2014). The Schwann cells and human umbilical cord mesenchymal stem cells had good attachment on the scaffolds, indicating good cell compatibility of the scaffolds. The porous structure of electrospun nanofibers and the roughness on the nanofibers can further enhance the adhesion of cells (Yang et al., 2015; Bagher et al., 2016). The orientation of the cells on the scaffolds was directed by the 320 nm nanofibers. It was reported that microfibers induce cell elongation across fibers while nanofibers can direct cell alignment along the fibers, which is a favorable characteristic for neural regeneration (Arslantunali et al., 2014). The advantage of the stable conductivity of our scaffolds will be confirmed by performing electrical stimulation on the cells in future experiments.

This work supports the use of aligned electrospun PLA/PPy nanofibrous scaffolds for the further development of nerve tissue engineering. Even though the scaffold showed good properties and cytocompatibility, the work is still at the primary stage of neural tissue engineering. More investigations need to be performed to confirm its regeneration effect when used *in vivo*.

In conclusion, we fabricated a scaffold for nerve tissue engineering and performed a primary investigation on formation of the material and its cytocompatibility. Our findings provide guidance for scaffold fabrication and contribute to the development of nerve tissue regeneration technology.

Acknowledgments: *We thank Cell Facility in Tsinghua Center of Biomedical Analysis for the assistance of using Zeiss LSM 710 instrument.*
Author contributions: *XDS and JP designed the study and wrote the paper. JFZ and YGW were in charge of the performance, collection, analysis and interpretation of data, and wrote the paper. LC and ZW participated in the experiments and provided technical support. All authors approved the final version of the paper.*
Conflicts of interest: *None declared.*
Plagiarism check: *This paper was screened twice using CrossCheck to verify originality before publication.*
Peer review: *This paper was double-blinded and stringently reviewed by international expert reviewers.*

References

Arslantunali D, Dursun T, Yucel D, Hasirci N, Hasirci V (2014) Peripheral nerve conduits: technology update. Med Devices (Auckl) 7:405-424.

Bagher Z, Ebrahimi-Barough S, Azami M, Safa M, Joghataei MT (2016) Cellular activity of Wharton's Jelly-derived mesenchymal stem cells on electrospun fibrous and solvent-cast film scaffolds. J Biomed Mater Res A 104:218-226.

Corey JM, Lin DY, Mycek KB, Chen Q, Samuel S, Feldman EL, Martin DC (2007) Aligned electrospun nanofibers specify the direction of dorsal root ganglia neurite growth. J Biomed Mater Res A 83:636-645.

El Omar R, Beroud J, Stoltz JF, Menu P, Velot E, Decot V (2014) Umbilical cord mesenchymal stem cells: the new gold standard for mesenchymal stem cell-based therapies? Tissue Eng Part B Rev 20:523-544.

Gu Y, Ji Y, Zhao Y, Liu Y, Ding F, Gu X, Yang Y (2012) The influence of substrate stiffness on the behavior and functions of Schwann cells in culture. Biomaterials 33:6672-6681.

Guo ZY, Sun X, Xu Xl, Peng J, Wang Y (2015) Human umbilical cord mesenchymal stem cells promote peripheral nerve repair via paracrine mechanisms. Neural Regen Res 10:651-658.

Hohman MM, Shin M, Rutledge G, Brenner MP (2001a) Electrospinning and electrically forced jets. II. Applications. Phys Fluids 13:2221-2236.

Hohman MM, Shin M, Rutledge G, Brenner MP (2001b) Electrospinning and electrically forced jets. I. Stability theory. Phys Fluids 13:2201-2220.

Hu AJ, Zuo BQ, Zhang F, Lan Q, Zhang HX (2012) Electrospun silk fibroin nanofibers promote Schwann cell adhesion, growth and proliferation. Neural Regen Res 7:1171-1178.

Kai D, Prabhakaran MP, Jin G, Ramakrishna S (2011) Polypyrrole-contained electrospun conductive nanofibrous membranes for cardiac tissue engineering. J Biomed Mater Res A 99:376-385.

Kim YT, Haftel VK, Kumar S, Bellamkonda RV (2008) The role of aligned polymer fiber-based constructs in the bridging long peripheral nerve gaps. Biomaterials 29:3117-3127.

Li QH, Zhou QH, Deng D, Yu QZ, Gu L, Gong KD, Xu KH (2013) Enhanced thermal and electrical properties of poly (D,L-lactide)/multi-walled carbon nanotubes composites by in-situ polymerization. Trans Nonferrous Met Soc China 23:1421-1427.

Liu X, Chen J, Gilmore KJ, Higgins MJ, Liu Y, Wallace GG (2010) Guidance of neurite outgrowth on aligned electrospun polypyrrole/poly(-styrene-β-isobutylene-β-styrene) fiber platforms. J Biomed Mater Res A 94:1004-1011.

Liu Y, He JH, Yu JY, Zeng HM (2008) Controlling numbers and sizes of beads in electrospun nanofibers. Polym Int 57:632-636.

Meng S, Rouabhia M, Shi G, Zhang Z (2008) Heparin dopant increases the electrical stability, cell adhesion, and growth of conducting polypyrrole/poly(L,L-lactide) composites. J Biomed Mater Res A 87:332-344.

Murugan R, Ramakrishna S (2007) Design strategies of tissue engineering scaffolds with controlled fiber orientation. Tissue Eng 13:1845-1866.

Pelto J, Björninen M, Pälli A, Talvitie E, Hyttinen J, Mannerström B, Suuronen Seppanen R, Kellomäki M, Miettinen S, Haimi S (2013) Novel polypyrrole-coated polylactide scaffolds enhance adipose stem cell proliferation and early osteogenic differentiation. Tissue Eng Part A 19:882-892.

Ramanaviciene A, Kausaite A, Tautkus S, Ramanavicius A (2007) Biocompatibility of polypyrrole particles: an in-vivo study in mice. J Pharm Pharmacol 59:311-315.

Schmidt CE, Leach JB (2003) Neural tissue engineering: strategies for repair and regeneration. Annu Rev Biomed Eng 5:293-347.

Shao S, Zhou S, Li L, Li J, Luo C, Wang J, Li X, Weng J (2011) Osteoblast function on electrically conductive electrospun PLA/MWCNTs nanofibers. Biomaterials 32:2821-2833.

Sharma AD, Zbarska S, Petersen EM, Marti ME, Mallapragada SK, Sakaguchi DS (2016) Oriented growth and transdifferentiation of mesenchymal stem cells towards a Schwann cell fate on micropatterned substrates. J Biosci Bioeng 121:325-335.

Shi G, Rouabhia M, Wang Z, Dao LH, Zhang Z (2004) A novel electrically conductive and biodegradable composite made of polypyrrole nanoparticles and polylactide. Biomaterials 25:2477-2488.

Shin YM, Hohman MM, Brenner MP, Rutledge GC (2001) Electrospinning: A whipping fluid jet generates submicron polymer fibers. Appl Phys Lett 78:1149-1151.

Stewart EM, Liu X, Clark GM, Kapsa RM, Wallace GG (2012) Inhibition of smooth muscle cell adhesion and proliferation on heparin-doped polypyrrole. Acta Biomater 8:194-200.

Sudwilai T, Ng JJ, Boonkrai C, Israsena N, Chuangchote S, Supaphol P (2014) Polypyrrole-coated electrospun poly(lactic acid) fibrous scaffold: effects of coating on electrical conductivity and neural cell growth. J Biomater Sci Polym Ed 25:1240-1252.

Wang X, Gu X, Yuan C, Chen S, Zhang P, Zhang T, Yao J, Chen F, Chen G (2004a) Evaluation of biocompatibility of polypyrrole in vitro and in vivo. J Biomed Mater Res A 68:411-422.

Wang Y, Li ZW, Luo M, Li YJ, Zhang KQ (2015a) Biological conduits combining bone marrow mesenchymal stem cells and extracellular matrix to treat long-segment sciatic nerve defects. Neural Regen Res 10:965-971.

Wang YL, Gu XM, Kong Y, Feng QL, Yang YM (2015b) Electrospun and woven silk fibroin/poly(lactic-co-glycolic acid) nerve guidance conduits for repairing peripheral nerve injury. Neural Regen Res 10:1635-1642.

Wang Z, Roberge C, Wan Y, Dao LH, Guidoin R, Zhang Z (2003) A biodegradable electrical bioconductor made of polypyrrole nanoparticle/poly(D,L-lactide) composite: A preliminary in vitro biostability study. J Biomed Mater Res A 66:738-746.

Wang Z, Roberge C, Dao LH, Wan Y, Shi G, Rouabhia M, Guidoin R, Zhang Z (2004b) In vivo evaluation of a novel electrically conductive polypyrrole/poly(D,L-lactide) composite and polypyrrole-coated poly(D,L-lactide-co-glycolide) membranes. J Biomed Mater Res A 70:28-38.

Xie J, MacEwan MR, Schwartz AG, Xia Y (2010) Electrospun nanofibers for neural tissue engineering. Nanoscale 2:35-44.

Xie J, Liu W, MacEwan MR, Bridgman PC, Xia Y (2014) Neurite outgrowth on electrospun nanofibers with uniaxial alignment: the effects of fiber density, surface coating, and supporting substrate. ACS Nano 8:1878-1885.

Xu H, Holzwarth JM, Yan Y, Xu P, Zheng H, Yin Y, Li S, Ma PX (2014) Conductive PPY/PDLLA conduit for peripheral nerve regeneration. Biomaterials 35:225-235.

Xu Y, Zhang Z, Chen X, Li R, Li D, Feng S (2016) A silk fibroin/collagen nerve scaffold seeded with a co-culture of schwann cells and adipose-derived stem cells for sciatic nerve regeneration. PLoS One 11:e0147184.

Yang A, Huang Z, Yin G, Pu X (2015) Fabrication of aligned, porous and conductive fibers and their effects on cell adhesion and guidance. Colloids Surf B Biointerfaces 134:469-474.

Yu QZ, Xu SL, Zhang KH, Shan YM (2013) Multi-porous electroactive poly(L-lactic acid)/polypyrrole composite micro/nano fibrous scaffolds promote neurite outgrowth in PC12 cells. Neural Regen Res 8:31-38.

Yuan N, Tian W, Sun L, Yuan RY, Tao JF, Chen DF (2014) Neural stem cell transplantation in a double-layer collagen membrane with unequal pore sizes for spinal cord injury repair. Neural Regen Res 9:1014-1019.

Zhang BG, Quigley AF, Myers DE, Wallace GG, Kapsa RM, Choong PF (2014a) Recent advances in nerve tissue engineering. Int J Artif Organs 37:277-291.

Zhang J, Qiu K, Sun B, Fang J, Zhang K, Ei-Hamshary H, Al-Deyab SS, Mo X (2014b) The aligned core-sheath nanofibers with electrical conductivity for neural tissue engineering. J Mater Chem B 2:7945-7954.

Zhang MJ, Sun JJ, Qian L, Liu Z, Zhang Z, Cao W, Li W, Xu Y (2011) Human umbilical mesenchymal stem cells enhance the expression of neurotrophic factors and protect ataxic mice. Brain Res 1402:122-131.

Zhang N, Yan H, Wen X (2005) Tissue-engineering approaches for axonal guidance. Brain Res Rev 49:48-64.

Zhang P, Lu X, Chen J, Chen Z (2014c) Schwann cells originating from skin-derived precursors promote peripheral nerve regeneration in rats. Neural Regen Res 9:1696-1702.

Zhang Z, Rouabhia M, Wang Z, Roberge C, Shi G, Roche P, Li J, Dao LH (2007) Electrically conductive biodegradable polymer composite for nerve regeneration: electricity-stimulated neurite outgrowth and axon regeneration. Artif Organs 31:13-22.

Zong X, Kim K, Fang D, Ran S, Hsiao BS, Chu B (2002) Structure and process relationship of electrospun bioabsorbable nanofiber membranes. Polymer 43:4403-4412.

Copyedited by Allen J, Frenchman B, Yu J, Li CH, Li JY, Song LP, Zhao M